Research Article

Ayad Mohammed Nattah*, Asia Mishaal Salim and Nawal Mohammed Dawood

Influence of nano chromium addition on the corrosion and erosion–corrosion behavior of cupronickel 70/30 alloy in seawater

https://doi.org/10.1515/eng-2022-0491
received April 15, 2023; accepted July 17, 2023

Abstract: Cupronickel alloys have found widespread use in various applications such as heat exchangers, refrigeration systems, equipment, pumps, and pipes. However, the inherent structure of cupronickel alone may not be able to withstand certain aggressive environments effectively. To address this issue, the mechanical properties and corrosion resistance of cupronickel alloys can be enhanced by carefully selecting the appropriate alloying compositions. The addition of nano chromium (20 nm) has been proposed as a means of designing cupronickel alloys with improved performance. In the present study, corrosion and erosion–corrosion behaviors of cupronickel 70/30 alloys produced by the casting method without and with three different additions of nano Cr (1, 1.2, and 1.5 wt%) were investigated. The prepared specimens were subjected to electrochemical tests in 3.5 wt% sodium chloride solutions to evaluate their corrosion behavior. Additionally, an erosion–corrosion test was conducted at an impact angle of 90°, using a slurry solution containing 1 wt% SiO_2 sand in 3.5 wt% NaCl solution as the erodent. The specimens were comprehensively characterized using scanning electron microscopy, energy-dispersive X-ray spectroscopy, and X-ray diffraction techniques. The surfaces of the alloy specimens exhibited superficial attacks, but no pits were observed. Moreover, the surfaces developed a greenish coloration. The electrochemical tests conducted using saline solution revealed that the corrosivity of the cupronickel alloy with nano chromium addition varied from moderate to low, depending on the selected concentration. Despite undergoing corrosion in the saline environment, the modified cupronickel alloys demonstrated good resistance to this corrosive process. Therefore, they can be considered suitable for use in highly aggressive environments, such as in seawater capture systems. The erosion–corrosion test results indicated that the addition of nano chromium significantly enhanced the resistance of the specimens to erosion–corrosion. At 1.5 wt% Cr, the erosion–corrosion rate was reduced by 99.27%.

Keywords: alloying elements, cupronickel 70/30 alloy, corrosion behavior, structural changes

1 Introduction

For over 60 years, copper and copper–nickel alloys (known as cupronickels) have been utilized in seawater applications, such as heat exchangers, condensers, pipes, and pumps, thanks to their excellent corrosion resistance. Previous reports [1–4] have established that incorporating nickel into copper to form cupronickel alloys produces materials that are highly resistant to corrosion. As a result, cupronickel alloys have found use in constructing equipment for various chemical industry applications. The primary reason for the resistance of corrosion of cupronickel alloys is the creation of a protective oxide film developed on the surface. This film, composed of Cu_2O and CuO, acts as a barrier that prevents the corrosive medium from reaching the metal matrix, thus halting further corrosion. When nickel is added to the Cu_2O film, the corrosion rate of the alloy can be reduced even further [5–8].

In flowing conditions, well-formed corrosion product films can effectively resist fluid erosion–corrosion and shield the substrate metal. However, copper–nickel alloy tubes still experience premature failures worldwide, which is mainly due to the corrosion product films' breakdown in moving fluid. This illustrates the need to develop a more thorough comprehension of the creation and progression of copper–nickel alloy corrosion product films in a flowing environment. Micro-alloying is an effective means of improving the corrosion resistance of cupronickel alloys

* **Corresponding author: Ayad Mohammed Nattah,** Department of Metallurgical Engineering, University of Babylon, Babylon, Iraq, e-mail: ayadnatah@yahoo.com
Asia Mishaal Salim: Department of Technique Engineering, College of Engineering, Al-Furat Al-Awsat Technical University, Kufa, Iraq
Nawal Mohammed Dawood: Department of Metallurgical Engineering, University of Babylon, Babylon, Iraq

[9–12]. Chromium, a transition metal element, has similar electron configuration and atomic radius to Fe, Mn, and Ni [13], and is frequently employed as an alloying element to enhance the resistance of corrosion of alloys [14]. Studies on the role of Cr in iron- and aluminum-based alloys have been conducted [15,16]. Taher et al. [13] and Zhang et al. [17] examined the electrochemical properties of cupronickel alloys with various elements of alloying and discovered that Cr could decrease the corrosion rate and corrosion current density of the alloy. However, these investigations were unsuccessful in revealing the Cr evolution in the corrosion product film or provide a detailed explanation of the mechanism by which Cr enhances the corrosion resistance of cupronickel alloys. As a result, it is essential to examine the effect of nano-alloying Cr elements in enhancing the resistance of corrosion of cupronickel alloys.

This study aims to investigate the effect of chromium as an element for alloying in enhancing the corrosion resistance of specific nickel-base casted alloys. Chromium has been recognized as a critical component in various alloys, and this study seeks to examine its role in improving the alloys' corrosion resistance under different environmental conditions. To accurately measure the effect of Cr on corrosion resistance, a 3.5% NaCl solution was used to assess the corrosion resistance of Cr-free alloys and compare them to those with varying amounts of Cr content. In addition to corrosion resistance evaluation, microstructural analysis was conducted to provide further insights into the role of Cr.

2 Experimental work

2.1 Alloy preparation

To produce cupronickel alloys, an electrolytic grade ingot copper with a minimum purity of 99.995% was used. Nickel, with a purity of 99.85%, was obtained from anode plates, and 99.9% pure nano (20 nm) Cr was used as raw materials.

Melting was performed in an electric furnace with a 2 kg capacity clay–graphite crucible coated with zircon, using graphite for stirring or plunging alloying elements. All melts were conducted in an oxidizing atmosphere using a flux, and a coagulant was added to thicken the flux residues for skimming and to prevent slag entrainment in the metal stream.

The cupronickel alloys were melted by first charging the crucible with the necessary metals, then heating them within a temperature range of 1,280–1,350°C for cupronickel 70/30 alloy and Cr (1, 1.2, and 1.5 wt%)-modified cupronickel 70/30 alloy. Deoxidization was achieved by plunging deoxidizing manganese tubes into the melt. Once the slag coagulant cover was skimmed, the crucible was moved to the pouring area. The melting and casting process took between 100 and 120 min, depending on the charge or melt condition, and after pouring, the castings were left to cool in the molds for at least an hour before being shaken out. In order to prevent severe micro-segregation, or coring, during the solidification of the cupronickel alloys, the researchers employed a heat treatment process called homogenization.

This involved subjecting some test bars to a programmed heat furnace for a typical soaking time of 5 h [18]. The homogenization temperature was typically set slightly above the upper annealing range, usually within 50°C of the solidus temperature, and was determined to be approximately 1,050°C for all cupronickel alloys. By homogenizing the alloys in this way, the researchers were able to eliminate micro-segregation and achieve a more uniform structure. To achieve homogenization of cupronickel alloys, similar precautions as those used during annealing were employed.

This includes controlling the furnace atmosphere to manage surface and internal oxidation. However, it is important to note that heating the castings too quickly may cause segregated phases to liquefy, posing a significant risk. Therefore, castings should be carefully supported and heated gradually through the final 100°C. All prepared specimens plus additives in weight percentage are given in Table 1.

2.2 Electrochemical polarization measurements

2.2.1 Test specimens

A piece of 14 mm diameter specimen was cut from the cast alloys after heat treatments. The surface to be tested is ground with SiC papers of grades 180, 320, 500, 600, 800 and 1,000, respectively. This process was followed by two stages of polishing. The first stage used diamond paste having particles of 3 μm diameter, while the second stage used 1 μm diameter of diamond paste in order to obtain a good polished surface. The specimens were subjected to ultrasonic cleaning for 3 min after the above process to eliminate any residues that may have accumulated [19,20]. Afterward, the specimens were placed in a conventional polarization cell of 200 mL. The cell contained a platinum counter electrode, a working electrode, and a saturated calomel reference electrode, as shown in Figure 1.

Using an Autolab potentiostat, the curves of polarization were created by sweeping the voltage at a rate of

Table 1: Chemical composition of alloys investigated in this work

Synthesized composition	Specimen code	Analyzed composition (wt%)		
		Cu%	Ni%	Cr%
Cupronickel 70/30 alloy	A	Bal.	30	—
Cupronickel 70/30–1% Cr	B1	Bal.	30	1
Cupronickel 70/30–1.2% Cr	B1	Bal.	30	1.2
Cupronickel 70/30–1.5% Cr	B1	Bal.	30	1.5

60 mV/min over the range of −250 to +250 mV relative to the open-circuit voltage. The measurements were conducted at a temperature of 25°C without agitation, in a saline solution with 3.5 wt% NaCl.

The solution was prepared by adding appropriate quantities of NaCl to deionized water. The pH was maintained at 6.5 ± 0.5, and the test temperature was 27 ± 3°C. To ensure reproducibility, all measurements were repeated at least three times. The corrosion rate can be calculated using the following equation [21]:

$$\mathrm{CR} = 22.85 \times I_{\mathrm{corr}}, \tag{1}$$

where I_{corr} is the current density of corrosion.

2.2.2 Micro-hardness test

The Vickers micro-hardness test was performed on all specimens using a load of 500 g and a holding time of 20 s [22]. A light optical microscope with a magnification of ×200 was attached to the Vickers instrument to aid in the examination. Four readings were taken for each specimen to account for the possibility of surface pores affecting the hardness measurements. The measurements were taken automatically and recorded straight from the digital screen of the instrument.

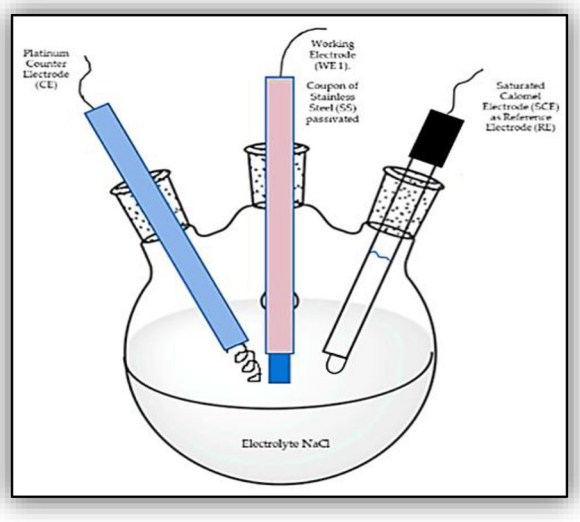

Figure 1: Corrosion test, conventional electrode cell (3.5 wt% NaCl).

2.2.3 Erosion–corrosion test

Erosion is a type of mechanical wear that results in material losses from solid surfaces due to the impact of solids, liquids, or gases. In this study, a device for testing erosion–corrosion was created according to ASTM (G 73) standards and is illustrated in Figure 2. The device includes a cylindrical plastic tank that is 50 cm tall and 30 cm in diameter. The specimen is positioned vertically in front of a jet nozzle (d = 0.75 mm), which is used to deliver various media at high pressures. A 1 HP Teflon chemical pump (single-phase electrical motor) is used to draw the media from the tank and maintain a distance of 10 mm between the specimen and the nozzle. The chemical pump and PVC plastic valves and pipe joints are designed to withstand the corrosive effects of the chemical solution and slurry [23].

2.2.4 X-Ray diffraction (XRD)

To examine the phases present in the as-cast cupronickel alloys, before and after exposure to a corrosive environment, a copper target was used, with Cu Kα radiation of wavelength 1.541838 Å, which was passed through a nickel filter. A start angle 2θ with 10° was used as this represented a position below the first peak. The test was stopped at 2θ of 90°.

3 Results and discussion

3.1 Microstructural characterization

The microstructure of ingots is affected highly by casting conditions. Figure 3a shows a longitudinal section from 13 mm in diameter of the 70/30 cupronickel billet. Some

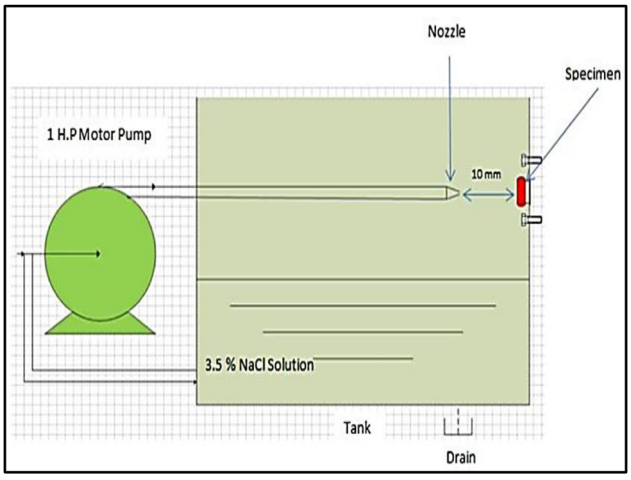

Figure 2: Erosion–corrosion device according to (G 73) ASTM.

dendrites appear to be equiaxed. Figure 3b shows a longitudinal section from 13 mm in diameter for the Cr-modified 70–30 cupronickel billet. The constituent chromium characterizes the dendrites in the homogenous cored structure with the solute elements filling up the interstices between the arms. Note that the dendrite arm spacing is the finest because the chromium addition leads to refining the structure. The Cr modified cupronickel has lower thermal conductivity than other cupronickel alloys. Energy-dispersive X-ray spectroscopy (EDS) analysis was used to examine the chemical composition of the formed phases/precipitates in cupronickel 70/30 alloy without and with 1.0, 1.2, and 1.5 wt% Cr alloys.

The results are depicted in Figure 4a and b and Table 2. Chromium appears as an additive to the cupronickel 70/30 alloy. The XRD results in Figure 5 reveal the phases present in the casted cupronickel 70/30 alloy. It can be observed that the structure of the casted alloy is almost identical, with only the peaks of the α matrix obtained for all prepared alloys.

However, the XRD examination does not provide information about the elements present in the alloy because it only scans the inter-metallics that occur within the structure, and not the elements forming the matrix. Figure 5a shows the diffraction pattern of the deflected X-rays of the cupronickel 70/30 alloy without the addition of chromium, while Figure 5b shows the diffraction pattern of the diffracted X-rays after the addition of 1.5% Cr. The comparison between the two figures makes it evident that chromium is not present in significant amounts, as its percentage falls below the diffraction limits of the XRD technique. Nonetheless, the impact of chromium on corrosion resistance is clearly noticeable.

3.2 Polarization curve measurements

The fresh surface of the four unetched specimens is depicted in Figure 5, which displays the anodic polarization curves. The corrosion potential (E_{corr}) of cupronickel 70/30–1.5% Cr alloy (about −165.84 mV) while cupronickel 70/30 alloy (about −183.67 mV), and the I_{corr} of Cupronickel 70/30–1.5% Cr alloy (9.86 μA/cm^2) is lower than that of cupronickel 70/30 alloy (20.82 μA/cm^2). The findings demonstrate that the cupronickel 70/30–1.5% Cr alloy is more susceptible to passivation compared to the cupronickel 70/30 alloy, indicating better corrosion resistance.

The reason behind this can be attributed to the fact that Cr exhibits a preferential passivation over Cu and has a lower passivation current density, as reported by previous studies [24,25]. Additionally, the shift in the corrosion

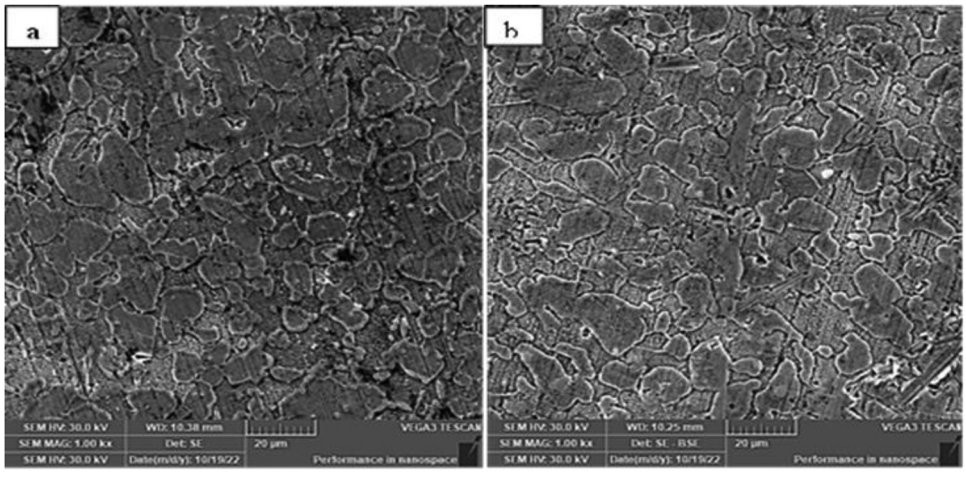

Figure 3: Scanning electron microscopy (SEM) of (a) cupronickel 70/30 alloy as cast and (b) cupronickel 70/30–1.5 wt% Cr alloy as cast.

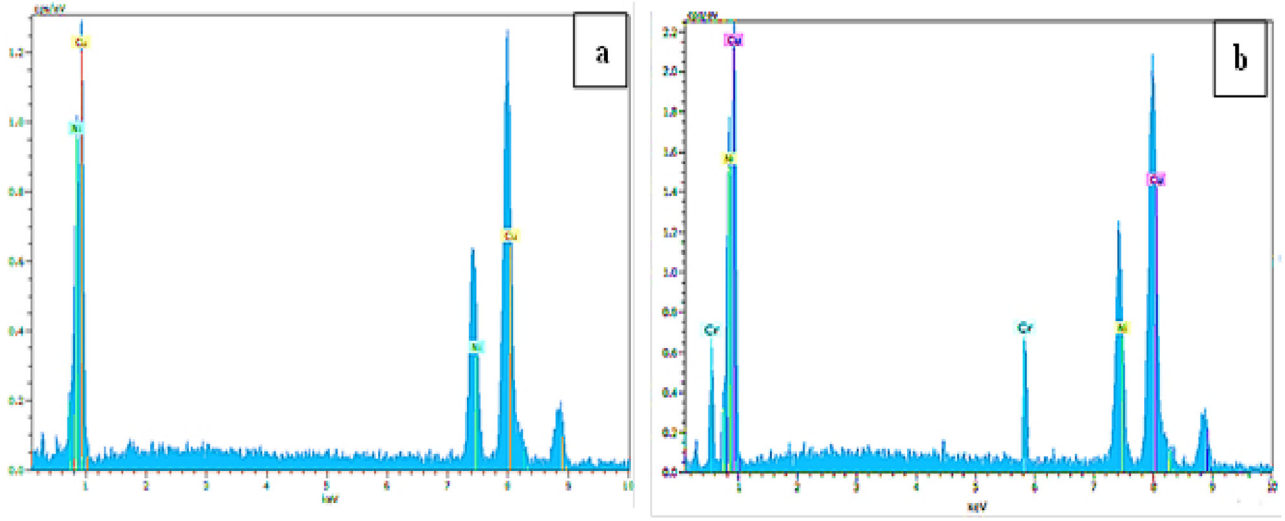

Figure 4: EDS analysis of (a) cupronickel 70/30 alloy as cast and (b) cupronickel 70/30–1.5 wt% Cr alloy as cast.

Table 2: EDS analysis of cupronickel 70/30 alloy as cast and cupronickel 70/30–1.5 wt% Cr alloy as cast

Synthesized composition	El	Norm (wt%)
Cupronickel 70/30 alloy	Cu	68.07
	Ni	31.93
	Total	100
Cupronickel 70/30–1.5% Cr	Cu	66.91
	Ni	31.76
	Cr	1.33
	Total	100

potentials to less negative values with increasing chromium content is consistent with the previous findings by Ekerenam et al. [24]. In addition, the study findings suggest that the alloys corroded by Cl− are prone to higher corrosion rates, possibly because of the greater number of active sites available for oxygen or adsorption of chlorine, which can be linked to the increased alloy surface roughness (Figure 6).

The electrochemical characteristic parameters, such as the corrosion potential (E_{corr}) and I_{corr} (μA/cm^2), are summarized in Table 3. The alloys' corrosion current density gradually decreases with increasing chromium content,

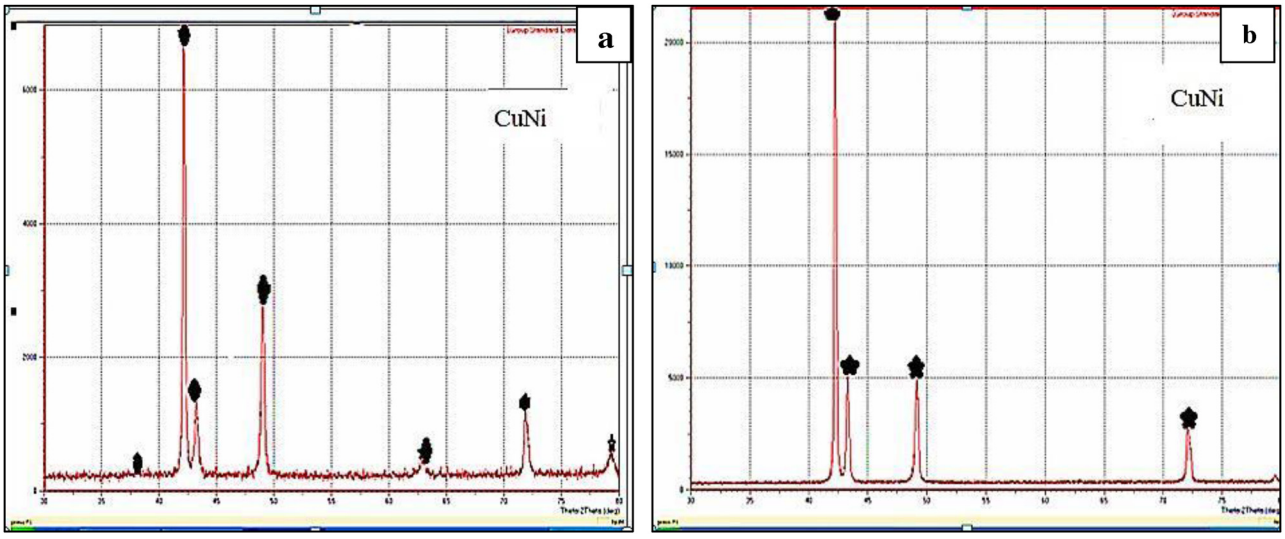

Figure 5: XRD analysis of (a) cupronickel 70/30 alloy as cast and (b) cupronickel 70/30–1.5 wt% Cr alloy as cast.

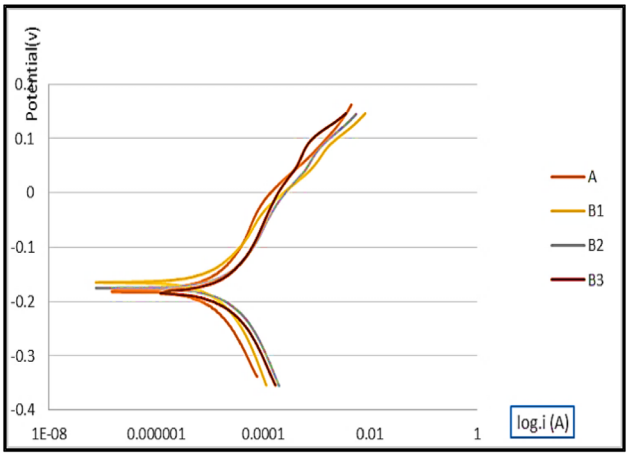

Figure 6: The polarization curves of cupronickel 70/30 without and with 1, 1.2, and 1.5 wt% Cr alloys after being introduced into a solution of 3.5 wt% NaCl.

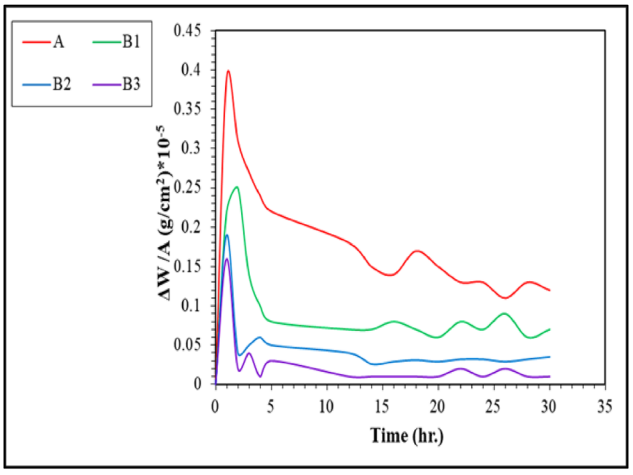

Figure 7: Erosion–corrosion rate for cupronickel 70/30 alloy–*x*% Cr.

which is thought to be due to the creation of a protective passive film [26]. These results suggest that the corrosion resistance of cupronickel 70/30–1.5% Cr is significantly better than that of the other alloys.

3.3 Microhardness result

According to the procedure mentioned in the study of Jabr and Dawood [27], the hardness of the cupronickel 70/30 alloy is 108 g/μm^2, which increases to 117, 120, and 128 g/μm^2 with the addition of 0.5, 1.2, and 1.5 wt% Cr, respectively. The most effective addition of Cr was found to be 1.5 wt%, which is attributed to the refinement of grains resulting from the inhibiting effects of the Cr element on grain growth within the solid solution.

3.4 Erosion–corrosion results

The results of the erosion–corrosion tests for cupronickel 70/30 alloy are shown in Figure 7. The tests were performed for 30 h with and without 0.5, 1, and 1.5 wt% in slurry solution (3.5 wt% NaCl with 1% SiO_2) at an impact angle of 90°. The data were collected every quarter of an hour during the first hour, every half hour during the second hour, and every hour after that. The specimen was cleaned with water and alcohol, dried under hot air, and the weight change was measured. Figure 7 shows that the curves fluctuate due to repeated formations and fractures of the protective surface layer. The erosion–corrosion rate decreases when this layer forms on the alloy's surface but increases when it breaks down, depending on the impact force and adhesion value on the alloy's surface [28]. During the initial immersion in the corrosive solution, the rate of erosion–corrosion (Figure 7) was higher due to the ease of removing the created corrosion and exposing a new metal surface to the corrosive media. Additionally, the area covered by the deformed zones that were produced by the impact of the erodent is directly proportional to the exposure time at a constant slurry speed [29]. By analyzing Figure 7, it can be observed that the addition of Cr elements to the base alloy results in a lower erosion–corrosion rate. This can be attributed to the increased alloy hardness with the addition of Cr, which was previously demonstrated, and this increase enhances their

Table 3: Characteristic parameters obtained from the polarization curves of four alloys after being exposed to 3.5 wt% NaCl solution

Specimen code	Current density (μA/cm^2)	E_{corr} (mV)	Corrosion rate (mm/year)
A	20.82	−183.67	0.475
B1	17.59	−181.65	0.401
B2	12.17	−175.73	0.278
B3	9.86	−165.84	0.225

Table 4: Erosion–corrosion rate and enhancement for the prepared alloy

Specimen code	Erosion–corrosion rate (g/cm^2 h)	Improvement (%)
A	0.137	—
B1	0.027	80.29
B2	0.005	96.35
B3	0.001	99.27

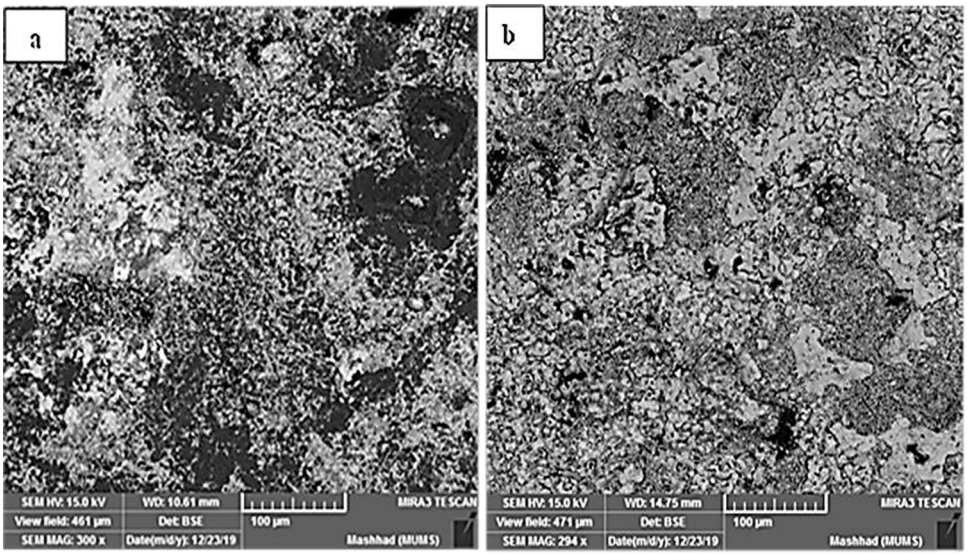

Figure 8: SEM analyses of surface morphology of (a) cupronickel 70/30 alloy and (b) cupronickel 70/30–1.5% Cr after erosion–corrosion test.

ability to resist erosion. Moreover, the cohesion of the protective oxide layer is improved by the addition of chromium. Table 4 displays the erosion–corrosion rate degradation and enhancement rates for the utilized alloys.

It can be observed from Figure 8a and b that the base alloy is more prone to erosion compared to the alloys with added Cr, as the base alloy (cupronickel 70/30 alloy) has lower hardness (HV of 108), while cupronickel 70/30–1.2% Cr has a higher microhardness measurement of 128.

4 Conclusion

This study aimed to investigate the corrosion and erosion–corrosion behavior and microstructures of casted cupronickel 70/30 alloys without and with 1, 1.2, and 1.5 wt% Cr addition. The findings of this study can be illustrated as follows:

1. The SEM images revealed the formation of pores within the structures and oxidized regions around the formed phases.
2. The XRD examinations identified the peaks belonging to alpha (α) matrix Cu–Ni phase in the cupronickel 70/30 alloys.
3. The addition of 1.2 wt% Cr to the base alloy resulted in a 526% reduction in the corrosion rate compared to the reference specimen in 3.5 wt% NaCl solution.
4. The cupronickel 70/30 alloy exhibited the highest current density, while the addition of Cr showed the lowest current density.
5. The addition of chromium at different percentages (1, 1.2, and 1.5 wt%) resulted in an improvement in hardness by 8%, 11%, and 19%, respectively.
6. With the addition of Cr, the rate of metal loss due to erosion is reduced, and the alloy demonstrates better resistance to erosion–corrosion. As the percentage of Cr addition increases, the alloy's resistance and stability also improve compared to the base alloy.

Acknowledgment: The Ministry of Higher Education and the University of Babylon are gratefully acknowledged. This research was carried out in the laboratory at the University of Babylon.

Funding information: The authors state no funding involved.

Author contributions: All authors have accepted responsibility for the entire content of this manuscript and approved its submission.

Conflict of interest: The authors state no conflict of interest.

Data availability statement: The authors declare that all data supporting the findings of this study are available within the article.

References

[1] Kapsalis C, Schmitt G, Feser R, Sagebiel B, Wilmes S, Macziek M. New investigations on critical wall shear stresses of CuNi alloys in natural and artificial seawater. Eurocorr-2011. Stockholm, Sweden: The Annual Congress of the European Federation of Corrosion; 2011. p. 1–14.

[2] Michel JH, Richardson I, Powell C, Phull B. Development of copper alloys for seawater service from traditional application to state-of-the art engineering. NACE International Corrosion Conference Proceedings. Houston; 2017. p. 9382.
[3] Mainier FB, Coelho AM, Barros EF. Corrosivity Evaluation of Copper-Nickel Alloy (90/10) in Pumps Used in Offshore Platforms for Seawater Pumping. Eng Tec Appl Sci Res. 2019;9(5):4636–9. doi: 10.48084/etasr.3016.
[4] Dawood NM, Abid Ali ARK. Influence of Titanium Additions on the Corrosion Behavior of Cu-Al-Ni Shape Memory Alloys. Mater Sci Forum. 2021;1021:55–67. doi: 10.4028/www.scientific.net/MSF.1021.55.
[5] Zhang D, Liu R, Liu Y, Xing S, Yang L, Wei E, et al. Multiscale characterization of seawater pipe erosion of B10 copper–nickel alloy welded joints. Sci Rep. 2022;12:2164. doi: 10.1038/s41598-022-06033-w.
[6] Jin T, Zhang W, Li N, Liu X, Han L, Dai W. Surface characterization and corrosion behavior of 90/10 copper-nickel alloy in marine environment. Materials (Basel). 2019;12(11):1869. doi: 10.3390/ma12111869.
[7] Zhang Y. Microstructure and Corrosion Behavior of as-cast 90Cu-10Ni Alloys with Different Yttrium Content. Int J Electrochem Sci. 2020;15:4161–78. doi: 10.20964/2020.05.47.
[8] Yuan SJ, Pehkonen SO. Surface characterization and corrosion behavior of 70/30 Cu–Ni alloy in pristine and sulfide-containing simulated seawater. Corros Sci. 2007;49:1276–304. doi: 10.1016/j.corsci.2006.07.003.
[9] Ijsseling FP. The application of the polarization resistance method to the study of the corrosion behavior of CuNil0Fe in seawater. Corros Sci. 1974;14(2):97–110. doi: 10.1016/S0010-938X(74)80048-X.
[10] Abraham GJ, Kain V, Dey GK. MIC failure of cupronickel condenser tube in fresh water application. Eng Fail Anal. 2009;16(3):934–43. doi: 10.1016/j.engfailanal.2008.08.007.
[11] Chandra K, Mahanti A, Singh AP, Kain V, Gujar HG. Microbiologically influenced corrosion of 70/30 cupronickel tubes of a heat-exchanger. Eng Fail Anal. 2019;105:1328–39. doi: 10.1016/j.engfailanal.2019.08.005.
[12] Chandra K, Kain V, Sinha SK, Gujar HG. Metallurgical investigation of a heat-exchanger tube of 70/30 cupronickel failed by fretting corrosion. Eng Fail Anal. 2020;116:104756. doi: 10.1016/j.engfailanal.2020.104756.
[13] Taher A, Jarjoura G, Kipouros GJ. Electrochemical behaviour of synthetic 90/10 Cu–Ni alloy containing alloying additions in marine environment. Corros Eng Sci Technol. 2013;48(1):71–80. doi: 10.1179/1743278212Y.0000000056.
[14] Zhu Z, Li S, Zhang R. Investigation of corrosion characteristics of Cu-10Ni-1.2Fe-*x*Mn (*x* = 0.53, 0.87, 32 1.19) alloy in 3.5% NaCl solution. RSC Adv. 2021;11(19):11318–28. doi: 10.1039/D0RA10678J.
[15] Sun J, Tang H, Wang C, Han Z, Li S. Effects of alloying elements and microstructure on stainless steel corrosion: A Review. Steel Res Int. 2022;93(5):2100450. doi: 10.1002/srin.202100450.
[16] Esquivel J, Gupta RK. Review-corrosion-resistant metastable al alloys: An overview of Corrosion Mechanisms. J Electrochem Soc. 2020;167(8):1504. doi: 10.1149/1945-7111/ab8a97.
[17] Zhang J, Wang Q, Wang Y, Wen L, Dong C. Highly corrosion-resistant $Cu_{70}(Ni,Fe,Mn,Cr)_{30}$ cupronickel designed using a cluster model for stable solid solutions. J Alloy Compd. 2010;505(1):179–82. doi: 10.1016/j.jallcom.2010.06.023.
[18] Abid Ali AR, Dawood NM. The Effect of Boron Addition on The Microstructure and Corrosion Resistance of Cu-Al-Ni Shape-Memory Alloys Prepared by Powder Technology. IOP Conf Ser: Mater Sci Eng. 2020;987:012028. doi: 10.1088/1757-899X/987/1/012028.
[19] Mainier FB, Figueiredo AAM, de Alencar Junior AAM, de Almeida BB. Proposal of the use sodium silicate as a corrosion inhibitor in hydrostatic testing of petroleum tanks using seawater. Int J Adv Eng Res Sci. 2018;5(6):33–8. doi: 10.22161/ijaers.5.6.6.
[20] Mainier FB, Farneze HN, Serrão LF, de Oliveira BT, Nani BF. Performance of stainless steel AISI 317L in hydrochloric acid with the addition of propargyl alcohol. Int J Electrochem Sci. 2018;13(4):3372–81. doi: 10.20964/2018.04.02.
[21] Dawood NM, Jasim TA. Electrodeposition of a Ni/TaC composite coating on 316L SS and its corrosion behavior in 3.5% sodium chloride solution. AIP Conf Proc. 2022;2660(1):20078. doi: 10.1063/5.0108470.
[22] Mutashar KA, Dawood NM. Improvement of Corrosion and Sliding Wear Behavior of Tin-Bronze Alloys Reinforced by ZrO_2 Particles Prepared via Powder Technology. Int J Mech Eng. 2022;7(1):1835–45.
[23] Dawood NM. Erosion-corrosion behavior of Al-20%Ni-Al_2O_3 metal matrix composites by stir casting. Mater Sci Forum. 2020;1002:161–74. doi: 10.4028/www.scientific.net/MSF.1002.161.
[24] Ekerenam OO, Ma A, Zheng Y, Emori W. Electrochemical behavior of three 90Cu-10Ni tubes from different manufacturers after immersion in 3.5% NaCl solution. J Mater Eng Perform. 2017;26:1701–16. doi: 10.1007/s11665-017-2566-1.
[25] Badawy WA, El-Rabiee MM, Helal NH, Nady H. Effect of nickel content on the electrochemical behavior of Cu–Al–Ni alloys in chloride free neutral solutions. Electrochim Acta. 2010;56(2):913–8. doi: 10.1016/j.electacta.2010.09.080.
[26] Dawood NM, Al-Sultani KF, Jasim HH. The role of zirconia additions on the microstructure and corrosion behavior of Ni-Cr dental alloys. Mater Res Exp. 2021;8(4):045404. doi: 10.1088/2053-1591/abfae4.
[27] Jabr NH, Dawood NM. Effect of Tungsten additions on Microstructure and Corrosion resistance of F75 alloy. J Phys: Conf Ser. 2021;1973(1):012135. doi: 10.1088/1742-6596/1973/1/012135.
[28] Dawood NM, Abid Ali ARK. Effect of Aging on Corrosion Behavior of Martensite Phase in Cu-Al-Ni Shape Memory Alloy. Key Eng Mater. 2022;911:96–102. doi: 10.4028/p-3jm065.
[29] Al Khaqani BH, Dawood NM, Ali OI. Erosions- Corrosion Behavior of (Al-Y2O3) Composite Prepared by Powder Metallurgy. J Mech Eng Res Dev. 2020;43(2):415–26.